Excess Molar Enthalpies of CO_2 + Acetone at Pressures from (9.00 to 18.00) MPa and Temperatures from (313.15 to 333.15) K

Fouad Zahran, Concepción Pando,* Juan A. R. Renuncio, and Albertina Cabañas

Departamento de Química Física I, Universidad Complutense, E-28040 Madrid, Spain

Mixtures of supercritical CO_2 and acetone are very often involved in supercritical fluid applications, and their thermodynamic properties are required to understand and design these processes. Excess molar enthalpies (H_m^E) for CO_2 + acetone mixtures were measured using an isothermal high-pressure flow calorimeter under conditions of temperature and pressure typically used in supercritical processes: pressures from (9.00 to 18.00) MPa and temperatures from (313.15 to 333.15) K. Mixtures showed exothermic mixing; excess molar enthalpies exhibited a minimum in the CO_2-rich region. The effects of pressure and temperature on the excess molar enthalpy of CO_2 + acetone are large. The most exothermic H_m^E values were observed for a coincident CO_2 mole fraction value of 0.771 at (323.15 and 333.15) K and 9.00 MPa: (−4176 and −4366) J·mol^{-1}, respectively. Two-phase vapor−liquid CO_2-rich regions are observed at (323.15 and 333.15) K and 9.00 MPa where H_m^E linearly varies with CO_2 mole fraction. For a given mole fraction and temperature, mixtures become more exothermic as pressure decreases. These trends were analyzed in terms of molecular interactions, phase equilibria, density, and critical parameters previously reported for CO_2 + acetone. Excess molar enthalpies here reported were correlated using the Peng−Robinson equation of state and the classical mixing rule with two binary interaction parameters. The influence of the thermal effects on the phase behavior of CO_2 + acetone mixtures formed in supercritical antisolvent precipitation experiments was discussed.

Introduction

The mixtures formed by supercritical carbon dioxide and organic solvents such as acetone have received considerable attention in the recent past due to the advantages of CO_2 over conventional organic solvents and its numerous applications in sustainable chemistry.[1] Supercritical carbon dioxide is often promoted as a green solvent since it is nontoxic, has low cost, is nonflammable, and allows operation at low temperatures and moderate pressures (T_c = 304.1 K, P_c = 7.38 MPa).[2] Carbon dioxide physical properties such as density, viscosity, and diffusion coefficient may be varied continuously from liquid-like to gas-like values by simply changing pressure and temperature conditions. Furthermore, a small amount of an organic polar solvent such as acetone may be added to the pure supercritical fluid to increase the solute solubility and/or selectivity in extraction applications.

Mixtures formed by supercritical CO_2 and acetone are also used in the micronization of solutes such as polymers, pharmaceutical compounds, explosives, and colorants. The so-called supercritical antisolvent precipitation (SAS) is based on using supercritical carbon dioxide as an antisolvent to induce controlled precipitation of solutes from their organic solvent solutions thanks to the relatively low solvent power of CO_2 for these solutes and its good miscibility with many organic solvents. SAS precipitation has been extensively used during the last years, and several reviews are available.[3−6] When the supercritical antisolvent dissolves in the organic solvent, the liquid experiences a volumetric expansion and becomes a bad solvent for the solute that precipitates from the solution in micro- and nanoparticles. Other typical polar organic solvents used are dimethylsulfoxide, *N*,*N*-dimethylformamide, dichloromethane, and *N*-methyl-2-pyrrolidone. On the other hand, CO_2-expanded solvents may also be used as reaction media.[7]

The numerous applications of mixtures formed by supercritical carbon dioxide and acetone have prompted researchers like Sala et al.[8] to undertake their study from a fundamental point of view. On the other hand, the physical and thermodynamic properties of the CO_2 + organic polar solvent mixtures are also required to understand and design supercritical fluid applications. Consequently, the high-pressure density and phase behavior and the volumetric expansion of CO_2 + acetone mixtures have received considerable attention in the last years.[9−23] However, not much attention has been paid to the heat evolved when supercritical CO_2 dissolves into the organic solvent. The excess molar enthalpies (H_m^E) at these conditions can be quite high. Thus, thermal effects during this process have an effect on the phase separation path and must be considered to optimize precipitation and reaction conditions. In a previous study,[24] H_m^E values for CO_2 + *N*-methyl-2-pyrrolidone mixtures were reported at (313.15 and 338.15) K and (9.48, 15.00, and 20.00) MPa. Furthermore, the relationship between thermal effects and phase behavior and coalescence phenomena observed in SAS micronization of several antibiotics was discussed. In this paper, we report excess molar enthalpies for the binary system CO_2 + acetone under conditions of temperature and pressure typically used in supercritical CO_2 applications: (313.15 and 323.15) K and (9.00, 12.00, 15.00, and 18.00) MPa and 333.15 K and (9.00 and 15.00) MPa. The excess enthalpy data for mixtures of CO_2 and acetone will be analyzed in terms of molecular interactions, phase equilibria, and density data and critical parameters. The influence of these thermal effects on the phase behavior of mixtures formed in the precipitation chamber in SAS experiments will be examined.

* Corresponding author. Phone: +34 91394 4304. Fax: +34 91394 4135. E-mail: pando@ quim.ucm.es.

10.1021/je100220c
Published on Web 07/13/2010

Experimental Section

The materials employed were CO_2 (Air Liquide, 99.98 % in mole) and acetone (Sigma-Aldrich, 99.9 % in mole). Commercial materials were used without further purification.

An isothermal high-pressure flow calorimeter (Hart Scientific model 7501) was used to perform H_m^E measurements. The calorimeter was first described by Christensen et al.,[25] and the experimental procedure is described elsewhere.[24] The reactants were pumped into the calorimetric cell by two thermostatted syringe pumps (model: LC-2600, ISCO) at constant flow rates. The temperature of the pumps was controlled within ± 0.02 K. Volume flow rates were selected to cover the entire concentration range. For each pump, the uncertainty in the volume flow rate was obtained by a previous calibration. The flow rate stability was ± 1 % over the total volume of the cylinder. The calorimetric cell was located in a silicon bath in which temperature was controlled within ± 0.001 K. A Peltier cooling device and a pulsed heater kept the cell under isothermal conditions. The pulse energy was determined by a previous heater calibration based on the Joule effect. The pressure was measured using a calibrated pressure transducer (Lucas Schaevitz, model P721-0001). A back-pressure regulator located outside the calorimeter kept the pressure within ± 0.01 MPa.

All runs were made in the steady-state fixed composition mode. Measurements at all the P and T conditions studied were carried out at total volume flow rates of (0.0014 and 0.0028) $cm^3 \cdot s^{-1}$. The CO_2 mole fraction range is covered by combining adequate values for the flow rates of the two pumps at these total volume flow rates. Also, the coincidence within the experimental error of results obtained using different total flow rates is an indication of equilibrium conditions in the calorimeter. The volume flow rates were converted to molar flow rates using the densities and molar masses. CO_2 densities at the temperature and pressure of the pumps were obtained from NIST webbook.[26] Acetone densities were obtained from the Tait equation provided by Adams and Laidler.[27] Since densities are affected by temperature and pressure changes, the error in molar flow rates was derived taking into account contributions from variations in volume flow rates, pressure, and pumps temperature. The mole fraction precision is based on the error in molar flow rates and was estimated to be better than ± 0.001. The error in H_m^E was obtained taking into account contributions from molar flow rates, pulse energy, and frequency and was estimated to be ± 1 % or at least ± 1 $J \cdot mol^{-1}$. Periodically, H_m^E values obtained using this calorimeter for the ethanol + H_2O system at 323.15 K and 15.00 MPa were compared to those previously reported by Ott et al.[28] This set of data has been proposed as a reference for isothermal dilution and flow calorimeters.[29]

Results and Discussion

H_m^E data for the binary system [$CO_2(x)$ + acetone$(1 - x)$] were determined at (313.15 and 323.15) K and (9.00, 12.00, 15.00, and 18.00) MPa as well as at 333.15 K and (9.00 and 15.00) MPa over the entire composition range and are given in Table 1. Figures 1 to 3 show plots of H_m^E vs CO_2 mole fraction at (313.15, 323.15, and 333.15) K, respectively. For comparison purposes, the same scale has been used for H_m^E in Figures 1 to 3.

Similar trends are observed for the variation of H_m^E with mole fraction and pressure. For a given mole fraction and temperature, mixtures become increasingly exothermic as the pressure decreases. At each condition of temperature and pressure, excess molar enthalpies exhibit a minimum in the CO_2-rich region. As the temperature increases for a given mole fraction and pressure, mixtures show more exothermic mixing. The most exothermic H_m^E values were observed at 9.00 MPa and (323.15 and 333.15) K. Minimum values of

Table 1. Excess Molar Enthalpy, H_m^E, for the Binary System [$CO_2(x)$ + Acetone$(1 - x)$]

x	H_m^E / $J \cdot mol^{-1}$	x	H_m^E / $J \cdot mol^{-1}$	x	H_m^E / $J \cdot mol^{-1}$
T/K = 313.15; P/MPa = 9.00					
0.095	−454	0.507	−2023	0.900	−2038
0.180	−935	0.586	−2226	0.938	−1736
0.246	−1202	0.662	−2288	0.969	−1202
0.337	−1494	0.771	−2366		
0.432	−1864	0.840	−2234		
T/K = 313.15, P/MPa = 12.00					
0.108	−323	0.395	−1049	0.781	−1201
0.189	−574	0.464	−1167	0.847	−1025
0.258	−732	0.562	−1284	0.911	−736
0.332	−922	0.675	−1321	0.971	−256
T/K = 313.15, P/MPa = 15.00					
0.111	−277	0.530	−1000	0.852	−724
0.194	−457	0.586	−1021	0.913	−499
0.264	−621	0.647	−1019	0.943	−364
0.340	−760	0.719	−980	0.972	−191
0.456	−906	0.787	−887		
T/K = 313.15, P/MPa = 18.00					
0.114	−264	0.479	−846	0.855	−569
0.198	−417	0.577	−898	0.915	−383
0.269	−541	0.652	−919	0.956	−218
0.346	−672	0.724	−857		
0.410	−781	0.791	−722		
T/K = 323.15, P/MPa = 9.00					
0.102	−728	0.507	−3132	0.840	−4050
0.158	−1096	0.586	−3491	0.906	−3434
0.246	−1699	0.699	−4003	0.938	−2609
0.319	−2142	0.771	−4176	0.969	−1132
0.424	−2689	0.805	−4174		
T/K = 323.15, P/MPa = 12.00					
0.108	−403	0.438	−1471	0.801	−1719
0.209	−761	0.562	−1687	0.879	−1389
0.305	−1062	0.646	−1771	0.941	−933
0.351	−1213	0.747	−1796	0.971	−553
T/K = 323.15, P/MPa = 15.00					
0.111	−308	0.530	−1186	0.913	−651
0.194	−531	0.609	−1244	0.943	−490
0.264	−714	0.683	−1240	0.972	−265
0.359	−905	0.787	−1122		
0.473	−1118	0.852	−932		
T/K = 323.15, P/MPa = 18.00					
0.114	−271	0.577	−1039	0.915	−453
0.219	−518	0.652	−1025	0.944	−324
0.318	−729	0.724	−967	0.973	−186
0.410	−883	0.791	−857		
0.479	−974	0.855	−698		
T/K = 333.15, P/MPa = 9.00					
0.102	−753	0.424	−2938	0.771	−4366
0.180	−1309	0.507	−3347	0.807	−4196
0.246	−1776	0.625	−4010	0.906	−2031
0.337	−2389	0.699	−4272	0.938	−1210
T/K = 333.15, P/MPa = 15.00					
0.111	−371	0.609	−1524	0.915	−844
0.215	−677	0.683	−1558	0.943	−653
0.312	−941	0.753	−1505	0.972	−342
0.404	−1191	0.820	−1296		
0.489	−1363	0.883	−1039		

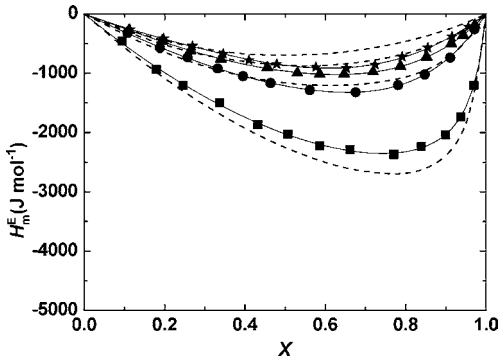

Figure 1. Excess molar enthalpies, H_m^E, for the binary system [$CO_2(x)$ + acetone$(1 - x)$] at 313.15 K and: ■, 9.00 MPa; ●, 12.00 MPa; ▲, 15.00 MPa; ★, 18.00 MPa; —, calculated using eq 3 and coefficients given in Table 2; - - -, calculated using the Peng−Robinson equation of state.[30]

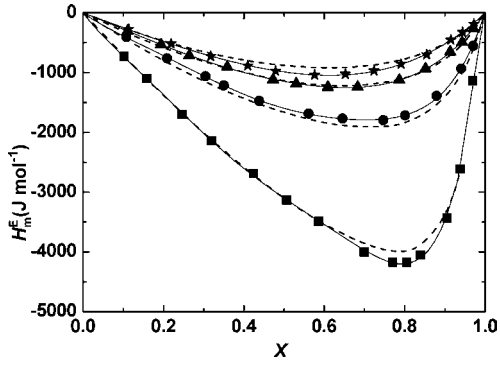

Figure 2. Excess molar enthalpies, H_m^E, for the binary system [$CO_2(x)$ + acetone$(1 - x)$] at 323.15 K and: ■, 9.00 MPa; ●, 12.00 MPa; ▲, 15.00 MPa; ★, 18.00 MPa; —, calculated using eq 3 and coefficients given in Table 2; - - -, calculated using the Peng−Robinson equation of state.[30]

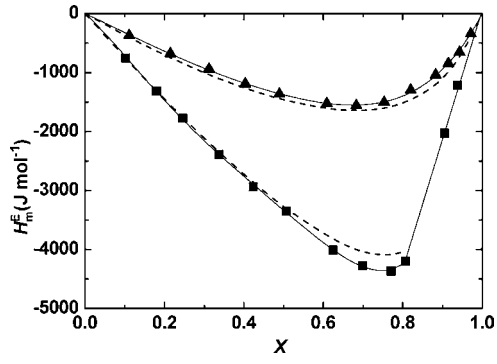

Figure 3. Excess molar enthalpies, H_m^E, for the binary system [$CO_2(x)$ + acetone$(1 - x)$] at 333.15 K and: ■, 9.00 MPa; ▲ 15.00 MPa; —, calculated using eq 3 and coefficients given in Table 2; - - -, calculated using the Peng−Robinson equation of state.[30]

(−4176 and −4366) J·mol^{-1} are reached, respectively, at these two temperatures for mixtures with a coincident CO_2 mole fraction value of 0.771. On the other hand, a linear section is observed in the H_m^E vs CO_2 mole fraction plot at these conditions of temperature and pressure. At 9.00 MPa and 323.15 K, this linear section is confined in the CO_2-rich region ($x > 0.931$). However, at 9.00 MPa and 333.15 K the linear section includes mixtures with $x > 0.788$. H_m^E varies linearly with CO_2 mole fraction due to the appearance of a two-phase region where a gaseous and a liquid mixture of fixed compositions, for a given condition of temperature and pressure, are in equilibrium. For a mixture of global composition x, the enthalpy effect in the two-phase region is the sum of two contributions due to the n_l moles of liquid mixture of composition x_l and n_v moles of vapor mixture of composition x_v

$$H_m^E = H_{m,l}^E n_l + H_{m,v}^E n_v \quad (1)$$

where $H_{m,l}^E$ is the excess molar enthalpy of the liquid mixture and $H_{m,v}^E$ is the excess molar enthalpy of the vapor mixture. Equation 1 may rewritten as[24]

$$H_m^E = H_{m,v}^E + \frac{x - x_v}{x_l - x_v}(H_{m,l}^E - H_{m,v}^E) \quad (2)$$

Since $H_{m,l}^E$, $H_{m,v}^E$, x_l, and x_v have constant values for each isotherm, the second member of eq 2 is a first-degree polynomial in x. When $x = x_l$, $H_m^E = H_{m,l}^E$, and when $x = x_v$, $H_m^E = H_{m,v}^E$. Therefore, the liquid- and vapor-phase compositions are shown to correspond to the x coordinates of the beginning and the end of the linear sections shown in Figures 2 and 3. A considerable amount of acetone may be present in the liquid mixture, but only a very small amount is dissolved in the vapor phase; in both linear sections, the CO_2 vapor-phase composition is very close to one and cannot be established from the calorimetric measurements. Two-phase regions do not appear for the other conditions of temperature and pressure studied in this paper. This is in agreement with high-pressure phase equilibria data previously reported for CO_2 + acetone at the same or similar temperatures.[9,13,16−19,21,23] The only exception is the data reported by Han et al. at 333.15 K.[20]

H_m^E data for [CO_2 (x) + acetone $(1 - x)$] were fitted to an (n, m) Padé function given by

$$H_m^E = x(1 - x)\frac{\sum_{i=0}^{n} A_i(2x - 1)^i}{1 + \sum_{j=1}^{m} B_j(2x - 1)^j} \quad (3)$$

where A_i and B_j are adjustable coefficients. A least-squares procedure was used to minimize deviations between experimental and calculated excess molar enthalpies. For those conditions of temperature and pressure where phase-splitting occurs, two different sets of coefficients are used to represent data in the two-phase and one-phase region, respectively. In the linear section, a (1, 2) Padé function with fixed values for the denominator coefficients, $B_1 = 0$ and $B_2 = -1$, may be used to keep the weight factor $x(1 - x)$. This results in a first-degree polynomial in the composition variable: the slope is $A_1/2$, and the zero intercept is $(A_0 - A_1)/4$. The H_m^E representation using eq 3 is shown in Figures 1 to 3. Table 2 lists values for the coefficients A_i and B_j and the standard deviation between experimental and calculated H_m^E values. The beginning of the linear section shown in Table 2 at (323.15 and 333.15) K and 9.00 MPa provides the value for the liquid-phase composition in the two-phase region.

The excess molar enthalpies of CO_2 + acetone were also calculated using the Peng−Robinson (PR) equation of state.[30]

Table 2. Coefficients A_i and B_j and Standard Deviation, σ, for Least-Squares Representation of H_m^E (J·mol^{-1}) for [CO_2 (x) + Acetone ($1 - x$)] at (313.15, 323.15, and 333.15) K using Equation 3

T	P									
K	MPa	interval	A_0	A_1	A_2	A_3	A_4	B_1	B_2	σ
313.15	9.00	$0 \le x \le 1$	−8088.28	2551.90	98.842	0	−26.213	−0.92178	0	7.3
	12.00	$0 \le x \le 1$	−4857.29	−2573.23	−1795.62	−1155.02	0	0	0	3.0
	15.00	$0 \le x \le 1$	−3858.17	−1754.55	−929.53	−659.27	0	0	0	1.8
	18.00	$0 \le x \le 1$	−3464.80	−1695.88	−296.08	441.31	0	0	0	2.7
323.15	9.00	$0 \le x \le 0.938$	−12389.48	−9127.38	−9809.38	−15590.29	−11435.57	0	0	9.7
		$0.938 \le x \le 1$	−83430.12	83644.97	0	0	0	0	−1	6.6
	12.00	$0 \le x \le 1$	−6385.06	−3743.81	−1717.40	−4039.31	−4543.33	0	0	5.5
	15.00	$0 \le x \le 1$	−4587.26	−2440.15	−1537.87	−1157.72	0	0	0	2.5
	18.00	$0 \le x \le 1$	−3951.52	−1883.26	−493.40	0	0	0	0	2.6
333.15	9.00	$0 \le x \le 0.807$	−13340.27	−11369.69	−12569.90	−8530.71	0	0	0	8.1
		$0.807 \le x \le 1$	−43631.78	43866.78	0	0	0	0	−1	4.6
	15.00	$0 \le x \le 1$	−5504.58	−3473.48	−2375.90	−1348.43	0	0	0	5.3

The excess molar enthalpy for a binary mixture is given by

$$H_m^E = H_m^R(\text{mixture}) - \sum_i x_i H_{m,i}^R \quad (4)$$

where H_m^R is the residual molar enthalpy of the mixture and $H_{m,i}^R$ is that of pure components. The residual molar enthalpy is given by

$$H_m^R = RT(z - 1) + \int_\infty^V \left[T\left(\frac{\partial P}{\partial T}\right)_V - P\right] dV \quad (5)$$

where z is the compressibility factor. The equation-of-state parameters a and b were evaluated for the mixtures using the classical mixing rule given by the equations

$$a = \sum_i \sum_j x_i x_j a_{ij}; \quad a_{ij} = (a_{ii}a_{jj})^{1/2}(1 - k_{ij})$$
$$b = \sum_i \sum_j x_i x_j b_{ij}; \quad b_{ij} = \frac{(b_{ii} + b_{jj})}{2}(1 - \delta_{ij}) \quad (6)$$

where $k_{ij} = k_{ji}$ and $\delta_{ij} = \delta_{ij}$ are binary interaction parameters. Values for the pure component parameters a and b were calculated using the acentric factor and the critical constants values given by Poling et al.[2] H_m^E data taken in the one-phase region at each of the three temperatures considered were simultaneously correlated using eqs 4 to 6. As was already discussed in the Experimental Section, the uncertainties in temperature, pressure, and composition are smaller than those of the excess molar enthalpies, and a least-squares-procedure was used to minimize relative deviations between experimental and calculated H_m^E. Table 3 lists values adopted by the binary interaction parameters k_{12} and δ_{12} and values for the standard deviation between experimental and calculated binary excess enthalpies, σ, for each condition of temperature and pressure. Results from the PR correlations are shown in Figures 1 to 3. A comparison of values for σ and the maximum absolute value of H_m^E for each condition of temperature and pressure indicates that relative deviations are larger for the 313.15 K correlation. The correlations are accurate at the higher temperatures of (323.15 and 333.15) K, thus allowing the prediction of excess molar enthalpies at temperatures and pressures in the T = (323.15 to 333.15) K and P = (9.00 to 18.00) MPa intervals.

Table 3. Densities of Carbon Dioxide,[26] Estimated Temperature Increments at Mixing, and Correlation of H_m^E Data for Carbon Dioxide + Acetone Binary Mixtures at (313.15, 323.15, and 333.15) K Using the PR Equation of State: Binary Parameters k_{12} and δ_{12} and Standard Deviation Between Experimental and Calculated Excess Enthalpies, σ

T	P	ρ_{CO2}	ΔT	PR		
K	MPa	g·cm^{-3}	K	k_{12}	δ_{12}	σ/J·mol^{-1}
313.15	9.00	0.4855	6.1	0.1127	0.0862	260
	12.00	0.7178	2.4			55
	15.00	0.7802	2.7			110
	18.00	0.8195	2.2			160
323.15	9.00	0.2850	11	0.0644	0.0478	78
	12.00	0.5847	5.1			110
	15.00	0.6998	3.1			36
	18.00	0.7571	2.5			62
333.15	9.00	0.2354	9.4	0.0405	0.0312	140
	15.00	0.6041	3.6			88

The large effects of pressure and temperature on the excess molar enthalpy values are related to changes in the state and densities of the pure components and their mixtures. The CO_2 + acetone system presents a liquid−gas type I diagram in the classification of Scott and van Konynenburg.[31] Figure 4 shows the P, T projection of CO_2 + acetone critical locus and the conditions of temperature and pressure for the experimental H_m^E data reported in this paper. The curve shown in Figure 4a covering the entire composition range was reported by Ziegler et al.[10] Several other authors reported critical data for CO_2-rich mixtures. In the T = (304 to 350) K interval, P_c varies linearly with T_c, and there is good agreement between literature critical data. The line shown in Figure 4b was obtained by a linear regression of data reported by Ziegler et al.,[10] Adrian and Maurer,[13] Reaves et al.,[15] Chen et al.,[18] and Chiu et al.[23] in this temperature interval. The state of the mixtures formed in the calorimeter (liquid, fluid, two-phase) may be established using Figure 4b and taking into account the critical composition and vapor−liquid equilibrium data.[9,13,16,9,21,23] At the conditions of H_m^E measurements, acetone is a liquid (T_c = 508.1 K, P_c = 4.70 MPa),[2] and its density does not change to a great extent with temperature and pressure.[27] However, carbon dioxide may be either a high-density (liquid-like) fluid or a low-density (gas-like) fluid. Densities of carbon dioxide are listed in Table 3. When carbon dioxide and acetone are mixed at 313.15 K and pressures greater than 9.00 MPa, carbon dioxide is a liquid-like fluid, and the resulting mixtures are mostly liquid. Critical data indicate that fluid mixtures are confined to a very narrow mole fraction range where $x > 0.975$. H_m^E values are moderately exothermic. The change-of-state contribution to H_m^E is small, and excess molar enthalpy values may be considered mainly the result of the molecular interaction contribution to H_m^E. Acetone presents a solvent structure dominated by dipole−dipole

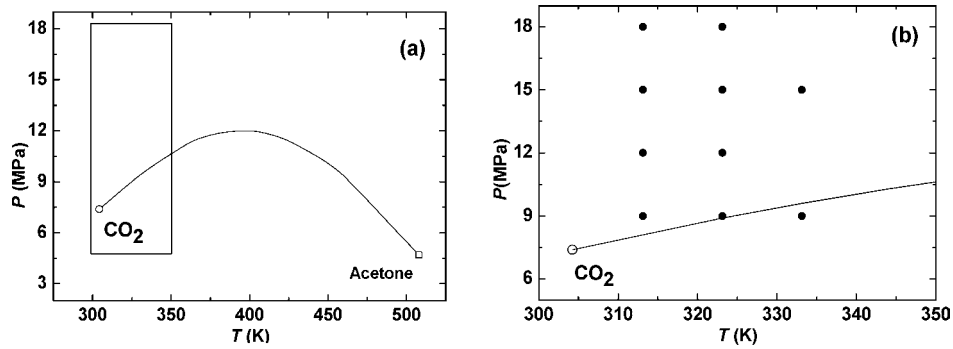

Figure 4. *P*, *T* projection of the CO_2 + acetone critical curve showing ○, the critical point of carbon dioxide and (a) locus reported by Ziegler et al.[10] and □, the critical point of acetone. (b) Locus in the CO_2-rich region based on data reported by Ziegler et al.,[10] Adrian and Maurer,[13] Reaves et al.,[15] Chen et al.,[18] and Chiu et al.[23]and the (*P*, *T*) coordinates where experimental data were taken, ●.

interactions that is disrupted upon mixing with carbon dioxide leading to an endothermic contribution to H_m^E. Moderately exothermic enthalpies are the result of a balance between the endothermic contribution and an exothermic one due to strong DMF−CO_2 interactions. This molecular interaction contribution may be expected to change only slightly with temperature and pressure in the intervals considered in this study. Mixing at 313.15 K and 9.00 MPa becomes considerably more exothermic as a result of combining a gas-like carbon dioxide with a liquid acetone to obtain liquid mixtures. The contribution to H_m^E due to intermolecular interactions is combined with another exothermic contribution due to the CO_2 change of state from that of a gas-like fluid to that of a liquid mixture component. This fluid condensation effect is even more pronounced at (323.15 or 333.15) K and 9.00 MPa when acetone is mixed with a fluid of very low density, and the resulting mixtures are a liquid or a gaseous and a liquid mixture in equilibrium. Fluid mixtures are also confined to a narrow mole fraction range at these conditions of temperature and pressure. Minimum values of (−4176 and −4366) $J \cdot mol^{-1}$ are reached for $x \approx 0.8$ at 9.00 MPa and (323.15 and 333.15) K, respectively. As the pressure is increased from (9.00 to 18.00) MPa at (323.15 or 333.15) K, carbon dioxide density increases, reaching values typical of a liquid at (15.00 or 18.00) MPa, and mixing becomes much less exothermic than that observed at the same temperature and 9.00 MPa.

Several authors[32−37] have pointed out that the phase behavior of CO_2 + organic solvent is one of the crucial factors governing the morphology and the mean size of particles obtained in the SAS process. The presence of the solute can induce modifications in the phase diagram. This is the case of polymers; however, when the solute has little interaction with carbon dioxide, the ternary phase diagram for the low solute concentrations usually employed in SAS is coincident with the binary one in the CO_2-rich region which is the region for mixtures involved in SAS.[33] Therefore, the mixtures formed in the precipitation chamber may be treated as binary CO_2 + organic solvent systems. In general, nanoparticles are obtained when the precipitation is carried out in the supercritical region. The uniformity of the resulting products becomes worse when the precipitation conditions approach the critical locus. Irregular microscale aggregated particles are formed in the vapor region, and both dense cake and spherical clusters are produced in the vapor−liquid region. The heat evolved when the supercritical CO_2 dissolves into the organic solution has an important role in the phase behavior. The temperature control in the precipitation chamber is not very precise, and the local temperature increase may lead to *T* and *P* conditions where phase splitting takes place. Since CO_2 is fed into the chamber at a flow rate much higher than that of the solution and the solute concentration is very low, the contribution to H_m^E due to solute interactions may be neglected, and the thermal effect in SAS experiments can be considered mainly due to the formation of CO_2 + acetone mixtures very rich in carbon dioxide ($x \geq 0.95$). Consequently, the temperature increase ΔT may be estimated using the H_m^E data reported in this paper. Since carbon dioxide is the predominant component in these mixtures, its isobaric heat capacity[38] was used to calculate the local temperature increase assuming an adiabatic process and using eq 3 to evaluate the heat evolved when a mole of mixture of composition $x = 0.95$ is formed. Values for ΔT thus obtained are shown in Table 3. An examination of these values together with literature vapor−liquid equilibrium data indicates how the heat evolved upon mixing affects the phase behavior. For instance, at 313.15 K and 9.00 MPa or at 323.15 K and 12.00 MPa carbon dioxide and acetone are completely miscible. However, a (6.1 or 5.1) K local temperature increase would approach precipitation conditions to the critical locus or even induce immiscibility for CO_2-rich mixtures formed in the SAS experiments, and the particle morphology would not correspond to that expected in a supercritical phase.

Conclusions

Excess molar enthalpies for mixtures of supercritical CO_2 and acetone were measured at (313.15 and 323.15) K and (9.00, 12.00, 15.00, and 18.00) MPa and 333.15 K and (9.00 and 15.00) MPa. The CO_2 + acetone system presents immiscibility at (323.15 and 333.15) K and 9.00 MPa; in this range, H_m^E varies linearly with mole fraction due to vapor−liquid equilibria.

The effects of pressure and temperature on the excess molar enthalpy are large. H_m^E values are exothermic at all the conditions of temperature and pressure studied and become extremely exothermic when low-density supercritical carbon dioxide is mixed with the liquid acetone and the resulting mixture is a liquid or a gaseous and a liquid mixture in equilibrium.

Excess molar enthalpies for CO_2 + acetone can be correlated using the PR equation of state and the classical mixing rule with two adjustable binary parameters for each temperature (T = (313.15, 323.15, and 333.15) K) in the P = (9.00 to 18.00) MPa interval.

Thermal effects in SAS experiments are shown to modify the phase behavior of CO_2 + acetone mixtures formed in the precipitation chamber thus affecting the morphology of the particles.

Literature Cited

(1) Beckmann, E. J. Supercritical and near-critical CO_2 in green chemical synthesis and processing. *J. Supercrit. Fluids* **2004**, *28*, 121–191.

(2) Poling, B. E.; Prausnitz, J. M.; O'Connell, J. P. *The properties of gases and liquids*; McGraw-Hill International ed.s: Singapore, 2001.
(3) Reverchon, E. Supercritical antisolvent precipitation of micro- and nano-particles. *J. Supercrit. Fluids* **1999**, *15*, 1–21.
(4) Jung, J.; Perrut, M. Particle design using supercritical fluids: Literature and patent survey. *J. Supercrit. Fluids* **2001**, *20*, 179–219.
(5) Pourmortazavi, S. M.; Hajimirsadeghi, S. S. Application of Supercritical Carbon Dioxide in Energetic Materials Processes: A Review. *Ind. Eng. Chem. Res.* **2005**, *44*, 6523–6533.
(6) Yeo, S. D.; Kiran, E. Formation of polymer particles with supercritical fluids: A review. *J. Supercrit. Fluids* **2005**, *34*, 287–308.
(7) Wei, M.; Musie, G. T.; Busch, D. H.; Subramaniam, B. CO_2-Expanded solvents: unique and versatile media for performing homogeneous catalytic oxidations. *J. Am. Chem. Soc.* **2002**, *124*, 2513–2517.
(8) Sala, S.; Danten, Y.; Ventosa, N.; Tassaing, T.; Besnard, M.; Veciana, J. Solute-solvent interactions governing preferential salvation phenomena of acetaminophen in CO_2 expanded solutions. A spectroscopic and theoretical study. *J. Supercrit. Fluids* **2006**, *38*, 295–305.
(9) Katayama, T.; Ohgaki, K.; Maekawa, G. G.; Nagano, T. Isothermal vapour-liquid equilibria of acetone-carbon dioxide and methanol-carbon dioxide at high pressures. *J. Chem. Eng. Jpn.* **1975**, *8*, 89–92.
(10) Ziegler, J. W.; Dorsey, J. G.; Chester, T. L.; Innis, D. P. Estimation of liquid-vapor critical loci for CO_2-solvent mixtures using a peak shape method. *Anal. Chem.* **1995**, *67*, 456–461.
(11) Day, C. Y.; Chang, C. J.; Chen, C. Y. Phase equilibrium of ethanol + CO_2 and acetone + CO_2 at elevated pressures. *J. Chem. Eng. Data* **1996**, *41*, 839–843.
(12) Pöhler, H.; Kiran, E. Volumetric properties of carbon dioxide + acetone at high pressures. *J. Chem. Eng. Data* **1997**, *42*, 379–383.
(13) Adrian, T.; Maurer, G. Solubility of carbon dioxide in acetone and propionic acid at temperatures between 298 and 333 K. *J. Chem. Eng. Data* **1997**, *42*, 668–672.
(14) Chang, C. J.; Day, C. Y.; Ko, C. M.; Chiu, K. L. Densities and *P-x-y* diagrams for carbon dioxide dissolution in methanol, ethanol, and acetone mixtures. *Fluid Phase Equilib.* **1997**, *131*, 243–258.
(15) Reaves, J. T.; Griffith, A. T.; Roberts, C. B. Critical properties of dilute carbon dioxide + entrainer and ethane + entrainer mixtures. *J. Chem. Eng. Data* **1998**, *43*, 683–686.
(16) Day, C. Y.; Chang, C. J.; Chen, C. Y. Phase equilibrium of ethanol + CO_2 and acetone + CO_2 at elevated pressures. *J. Chem. Eng. Data* **1999**, *44*, 365.
(17) Bamberger, A.; Maurer, G. High-pressure (vapour-liquid) equilibria in carbon dioxide + acetone or 2-propanol) at temperatures from 293 to 333 K. *J. Chem. Thermodyn.* **2000**, *32*, 685–700.
(18) Chen, J.; Wu, W.; Han, B.; Gao, L.; Mu, T.; Liu, Z.; Du, J. Phase behavior, densities, and isothermal compressibilities of CO_2 + pentane and CO_2 + acetone systems in various phase regions. *J. Chem. Eng. Data* **2003**, *48*, 1544–1548.
(19) Stievano, M.; Elvassore, N. High-pressure density and vapor-liquid equilibrium for the binary systems carbon dioxide-ethanol, carbon dioxide-acetone and carbon dioxide-dichloromethane. *J. Supercrit. Fluids* **2005**, *33*, 7–14.
(20) Han, F.; Xue, Y.; Tian, Y.; Zhao, X.; Chen, L. Vapor-liquid equilibria of the carbon dioxide + acetone system at pressures from (2.36 to 11.7) MPa and temperatures from (333.15 to 393.15) K. *J. Chem. Eng. Data* **2005**, *50*, 36–39.
(21) Lazzaroni, M. J.; Bush, D.; Brown, J. S.; Eckert, C. A. High-Pressure Vapor-Liquid Equilibria of Some Carbon Dioxide + Organic Binary Systems. *J. Chem. Eng. Data* **2005**, *50*, 60–65.
(22) Wu, W.; Ke, J.; Poliakoff, M. Phase boundaries of CO_2 + toluene, CO_2 + acetone, and CO_2 + ethanol at high temperatures and high pressures. *J. Chem. Eng. Data* **2006**, *51*, 1398–1403.
(23) Chiu, H. Y.; Lee, M. J.; Lin, H. Vapor-liquid phase boundaries of binary mixtures of carbon dioxide with ethanol and acetone. *J. Chem. Eng. Data* **2008**, *53*, 2393–2402.
(24) Dávila, M. J.; Cabañas, A.; Pando, C. Excess molar enthalpies for binary mixtures related to supercritical antisolvent precipitation: carbon dioxide + *N*-methyl-2-pyrrolidone. *J. Supercrit. Fluids* **2007**, *42*, 172–179.
(25) Christensen, J. J.; Hansen, L. D.; Izatt, R. M.; Eatough, D. J.; Hart, R. M. Isothermal flow calorimeter. *Rev. Sci. Instrum.* **1976**, *47*, 730–734.
(26) NIST Standard Reference Database Number 69, which can be accessed electronically through the NIST Chemistry Web Book (http://webbook.nist.gov/chemistry/).
(27) Adams, W. A.; Laidler, K. J. Effect of pressure and temperature on the structure of liquid acetone. *Can. J. Chem.* **1967**, *45*, 123–130.
(28) Ott, J. B.; Cornett, G. V.; Stouffer, C. E.; Woodfield, B. F.; Guanquan, C.; Christensen, J. J. Excess-enthalpies of (ethanol + water) at 323.15, 333.15, 348.15, and 373.15 K and from 0.4 to 15 MPa. *J. Chem. Thermodyn.* **1986**, *18*, 867–875.
(29) Sabbah, R.; Xu, A.; Chickos, J. S.; Planas-Leitão, M. L.; Roux, M. V.; Torres, L. A. Reference materials for calorimetry and differential thermal analysis. *Thermochim. Acta* **1999**, *331*, 93–204.
(30) Peng, D. Y.; Robinson, D. B. A new two-constant equation of state. *Ind. Eng. Chem. Fundam.* **1976**, *15*, 59–64.
(31) Scott, R. L.; van Konynenburg, P. H. Van der Waals and related models for hydrocarbon mixtures. *Discuss. Faraday Soc.* **1970**, *49*, 87–97.
(32) Reverchon, E.; Caputo, G.; De Marco, I. Role of Phase Behavior and Atomization in the Supercritical Antisolvent Precipitation. *Ind. Eng. Chem. Res.* **2003**, *42*, 6406–6414.
(33) Reverchon, E.; De Marco, I.; Torino, E. Nanoparticles production by supercritical antisolvent precipitation: A general interpretation. *J. Supercrit. Fluids* **2007**, *43*, 126–138.
(34) Chang, S. C.; Lee, M. J.; Lin, H. M. The influence of phase behaviour on the morphology of protein α-chymotrypsin prepared via a supercritical anti-solvent process. *J. Supercrit. Fluids* **2008**, *44*, 219–229.
(35) Chang, S. C.; Lee, M. J.; Lin, H. M. Role of phase behavior in micronization of lysozyme via a supercritical anti-solvent process. *Chem. Eng. J.* **2008**, *139*, 416–425.
(36) Martín, A.; Cocero, M. J. Micronization processes with supercritical fluids: fundamentals and mechanisms. *Adv. Drug Delivery Rev.* **2008**, *60*, 339–350.
(37) Reverchon, E.; Torino, E.; Dowy, S.; Brauer, A.; Leipertz, A. Interactions of phase equilibria, jet fluid dynamics and mass transfer during supercritical antisolvent micronization. *Chem. Eng. J.* **2010**, *156*, 446–458.
(38) Span, R.; Wagner, W. A new equation of state for carbon dioxide covering the fluid region from the triple-point temperature to 1100 K and pressures up to 800 MPa. *J. Phys. Chem. Ref. Data* **1996**, *25*, 1509–1596.

Received for review March 10, 2010. Accepted June 29, 2010. We gratefully acknowledge the financial support of the Santander-Universidad Complutense de Madrid, research project PR34/07-15789, and the Spanish Ministry of Education and Science (MEC), research project CTQ2009-09707. F.Z. thanks the E. U. for its support through an Erasmus Mundus University II predoctoral grant.

JE100220C